# Diagnostic Medical Image Processing

## Defect Pixel Interpolation

WS 2010/11

Joachim Hornegger, Dietrich Paulus, Markus Kowarschik

Lehrstuhl für Mustererkennung (Informatik 5)

Friedrich-Alexander-Universität Erlangen-Nürnberg

# Diagnostic Medical Image Processing

# Flat Panel Image Receptors

- replace image intensifier technology and film
- implied profound changes in radiology
- are well established in
  - digital radiography
  - cardiology
  - mammography

# Killer Applications of Flat Panel Detectors

With the introduction of flat panel detector technology, standard radiography systems could increase patient throughput and experienced a significant simplification of image archiving and image exchange with other hospitals and physicians.

Figure 1: Radiography system using flat panel detectors (image: Siemens Healthcare)

# Killer Applications of Flatpanel Detectors I

- **Cardiology:** In cardiology flat panel detectors where introduced in 2002.
- **Neuroradiology:** Biplane flat panel detector C-arm systems are available on the market since beginning of 2006.
- Flat panel detectors allow for 3-D reconstruction of static, low contrast objects using C-arm systems.

Figure 2: Cardiac system using a flat panel detector (left), biplane neuroradiology system (image: Siemens Healthcare)

# Killer Applications of Flatpanel Detectors II

The following images show examples of the contrast resolution achieved by today’s C-arm CT devices and algorithms.

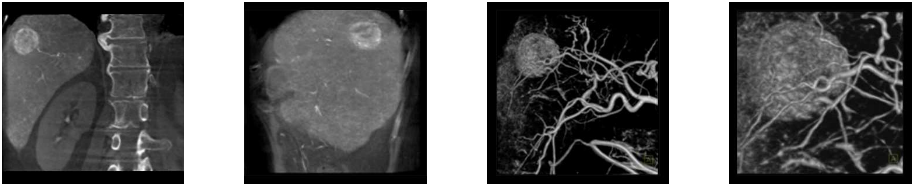

Figure 3: 3D low contrast C-arm reconstruction: Hepatocellular Carcinoma (image: Siemens Healthcare)

# Killer Applications of Flatpanel Detectors III

In **magnetic navigation systems** the catheter is directed by a magnetic field. The manual control of its orientation is based on X-ray images. Obviously it is impossible to operate an image intensifier in a magnetic field. Flat panel technology thus is mandatory.

Figure 4: Niobe system for magnetic navigation (image: Siemens Healthcare)

# Advantages of Flat Panel Detectors

- simple assembly and readout
- higher contrast resolution (high dynamic range)
- not sensitive to magnetic fields (no magnetic distortion)
- more robust with respect to under–/overexposure
- reduced space requirements (do not underestimate this advantage!)
- optimization of the clinical workflow
- mechanically rugged

# Disadvantages of Flat Panel Detectors

- relatively slow readout
- still very expensive technology
- high rejection rate in production
- elimination of defects with digital image processing
- still expensive technology (will change over time)

# Contrast Resolution

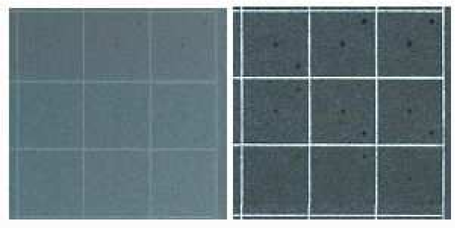

Figure 5: Higher contrast resolution using flat panel detectors: left image acquired on film, right image acquired with a digital detector (image: General Electrics)

# Goals of Flat Panel Design

- digital imaging in all areas of radiology, i.e. replace film and image intensifiers
- cost reduction in health care (elimination of film!)
- improved image quality
- waste minimum amount of incoming X-ray (fill factor ca. 40 %)
- area sizes more than 40cm $\times$ 40cm
- spatial resolution of pixels 100 $-$ 150$\mu$m

# Detective Quantum Efficiency

## Definition

The **detective quantum efficiency** (DQE) measures the decrease in SNR of a particular imaging system and is given by

$$DQE(f) = \frac{SNR^2(f)_{out}}{SNR^2(f)_{in}} \quad (1)$$

- theoretical foundations by Albert Rose in 1946
- *DQE* named after R. Clark Jones of Polaroid

# Flat Panel Detectors

Figure 6: Pixium 4600

Typical image data of a Pixium 4600:

- area: 43cm $\times$ 43cm
- resolution: 3121 $\times$ 3121
- pixel size: 143$\mu$m
- quantization: 14 bit (2 byte)

# Different Flat Panel Detectors

Figure 7: Examples of different detectors (left, middle) and the inside view

# Different Flat Panel Detectors

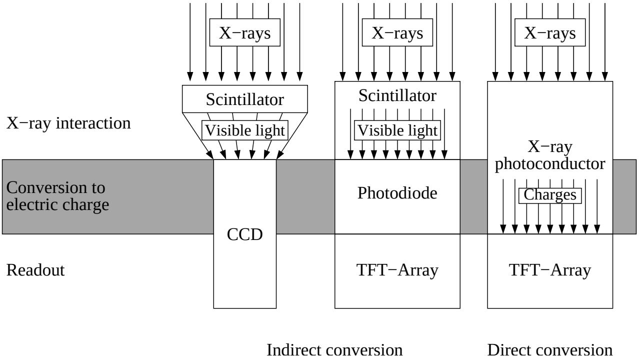


Figure 8: Different types of detectors

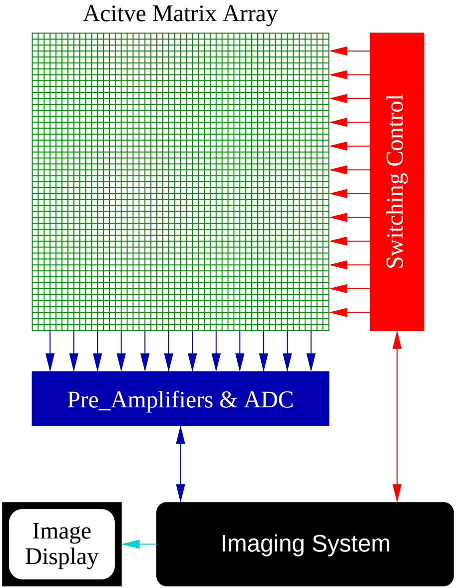


Figure 9: Structure of a flat panel detector

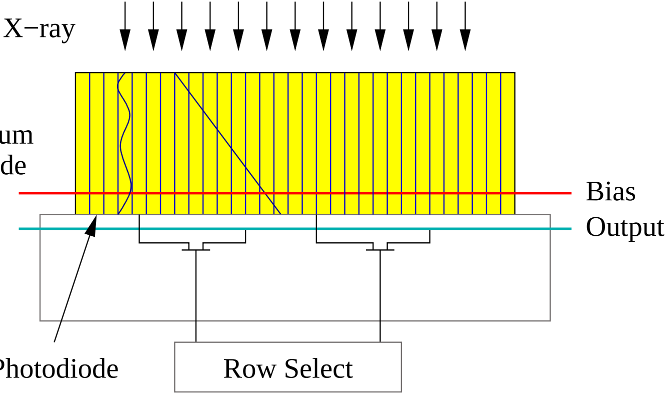


Figure 10: CsI based detectors

# Flat Panel Detector Readout

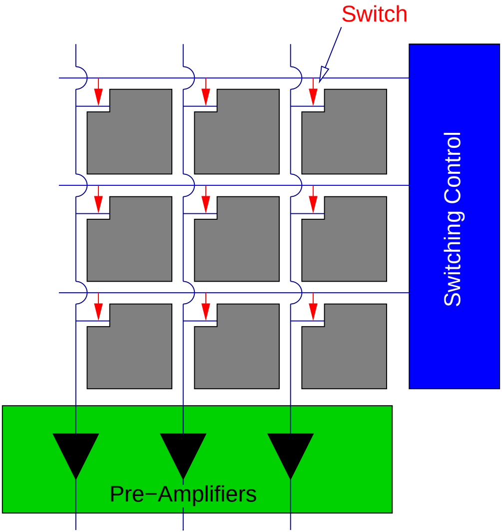


Figure 11: Construction principle of flat panel detector

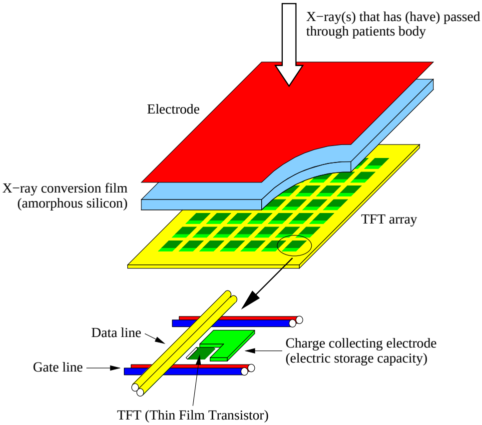


Figure 12: Direct conversion using amorphous silicon

# Artifacts of flat panel image receptors

- large detectors are composed by four detectors (butting cross)
- offset in intensities
- inactive pixels:
  - single pixels
  - pixel clusters
  - image columns
  - image rows

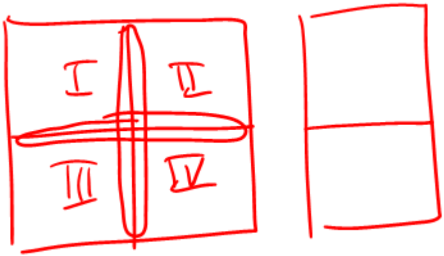

# Typical Pre-processing Problems

- offset and gain correction
- defect interpolation
- butting cross correction

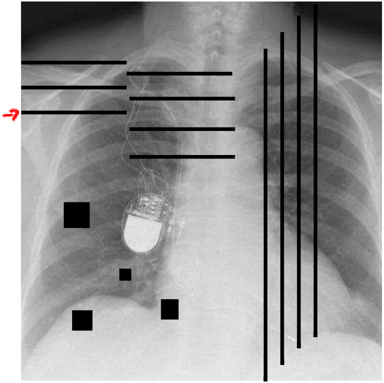

Figure 13: Thorax image with defect pixels

# Defect pixel interpolation

1. **Interpolation in spatial domain:**
   - non-adaptive linear filtering
   - non-linear filtering (like median)
   - suitable for small defect areas
   - unnatural appearance (amplified by post–processing)
2. **Interpolation in frequency domain:**
   - enforce band-limitation by bandpass filtering
   - defect interpolation corresponds to the deconvolution of defect and ideal image
   - binary defect image is computed in a calibration step
   - ideal image is multiplied with the binary defect image

# Butting Cross Artifact

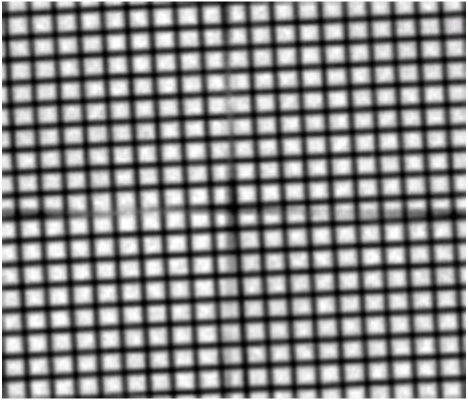

Figure 14: Artifacts appearing after butting cross correction

# Butting Cross Artifact

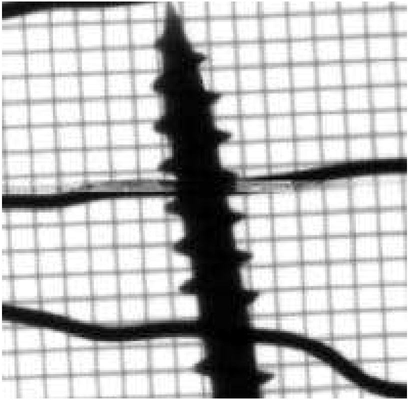

Figure 15: Artifacts caused by improper correction method

# Diagnostic Medical Image Processing

# Defect Pixels: Model

Defect pixels are caused by defect detector cells. The mathematical model for defect generation is just the multiplication of the original image with a defect mask:

- Let $f_{i,j}$ denote the intensity value at grid point $(i, j)$ of the **ideal image** $f$ that has no defect pixels
- Let $w_{i,j}$ denote the indicator value at $(i, j)$ where $w$ is **mask image** that indicates defect and uncorrupted pixels

$$w_{i,j} = \begin{cases} 0 & \text{if pixel is defect} \\ 1 & \text{otherwise} \end{cases}$$

- Let $g_{i,j}$ denote the intensity value at grid point $(i, j)$ of the **observed image** $g$ that is acquired with the flat panel detector that has defect pixels.

# Mathematical Modeling of Pixel Defects

By pixelwise multiplication of the ideal image with the mask image we get the observed image:

$$f_{i,j} \cdot w_{i,j} = g_{i,j} \Longleftrightarrow \boxed{f_{ij} = \frac{g_{ij}}{w_{ij}}} \qquad (2)$$


Figure 16: Ideal image (left) is multiplied with defect image mask (middle) and results in the output defect image (right)

# Defect Pixel interpolation in spatial domain

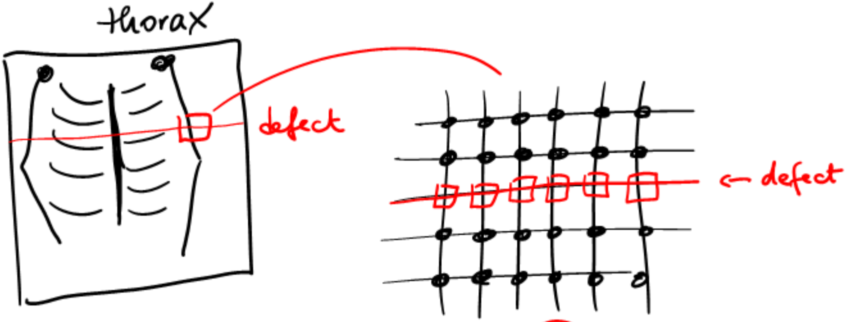


- spatial interpolation
- frequency domain interpolation

bilinear interpolation

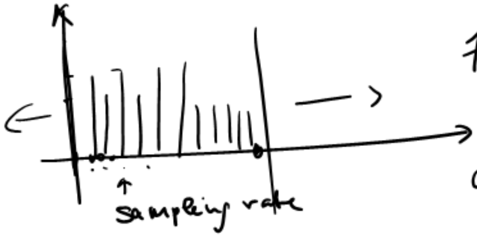


$$f(x) = \frac{a_0}{2} + \sum_{n \geq 1} a_n \cos nx + b_n \sin nx$$

$$\cos x + i \cdot \sin x = e^{ix}$$

$$\boxed{a_n = \frac{1}{\pi} \int_{-\pi}^{\pi} f(x) \cos nx \, dx}$$

# Defect Pixel Interpolation

For simplicity and without loss of generality we limit the following discussion to 1-D signals of length $N$ and use the following notation:

- discrete ideal signal: $f(n)$
- binary mask image: $w(n)$
- observed signal: $g(n)$

# Diagnostic Medical Image Processing

# Fourier Transform Revisited

1   i

The following discussions will heavily make use of the Fourier transform and its properties.
The Fourier transform of a 1-D signal is defined by

$\mathcal{O}(N \log N)$

$\xi = 0$

$$F(\xi) = \sum_{n=0}^{N-1} f(n) e^{\frac{-2\pi i n \xi}{N}}$$

$$M \begin{pmatrix} f(0) \\ f(1) \\ \vdots \\ f(N-1) \end{pmatrix} = \begin{pmatrix} F(0) \\ \vdots \\ F(N-1) \end{pmatrix}$$

# Defect Pixel Interpolation

$x^N - 1 \leq 0$

The algorithms for defect pixel interpolation apply three important properties of the Fourier transform or results related to the Fourier transform:

- Nyquist Shannon sampling theorem
- convolution theorem
- symmetry property Fourier transform of real signals

# Sampling Theorem

$f(n)$; $F(\xi) \equiv 0$, $\xi > B$

## Theorem

*Given the continuous function $f(n) \in \mathbb{R}, n \in \mathbb{R}$ with a limited bandwidth $B$, i.e. the Fourier transform of $f(n)$ satisfies $F(\xi) = 0$ for $\xi > B$. The interpolation using discrete sampling points allows the reconstruction of $f(n)$, if the function is sampled with a sampling rate that is larger than twice the bandwidth $B$, i.e.*

$$f_{sampling} > 2B$$

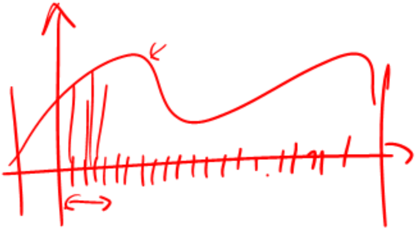

$$f(x) = \sum_k a_k \cos k\cancel{x} + b_k \sin kx$$

# Convolution Theorem

$f(\vec{x})$ is linear iff $\left.\begin{array}{l} f(\lambda \vec{x}) = \lambda f(\vec{x}) \\ f(\vec{x}+\vec{y}) = f(\vec{x}) + f(\vec{y}) \end{array}\right\} f\left(\sum_i \lambda_i \vec{x}_i\right) = \sum_i \lambda_i f(\vec{x}_i)$

## Theorem

**Convolution theorem**: *The convolution of two signals in the time domain, corresponds to a multiplication in the frequency domain:*

$$g(n) = \sum_{k=0}^{N-1} f(k)h(n-k) = f \star h$$

$$g(y) = \int f(x) \cdot h(y-x)\,dx$$

$$G(\xi) = F(\xi)H(\xi)$$

# Convolution Theorem

The Fourier transform of $f \star h$ is

n-k

$$
\begin{aligned}
FT(f \star h)(\xi) &= \overbrace{\sum_{n=0}^{N-1} \sum_{k=0}^{N-1} f(k)h(n-k)}^{g(n)} e^{\frac{-2\pi i n \xi}{N}} \\
&= \sum_{k=0}^{N-1} f(k) \sum_{n=0}^{N-1} h(n-k) e^{\frac{-2\pi i n \xi}{N}} \\
&= \underbrace{\sum_{k=0}^{N-1} f(k) e^{\frac{-2\pi i k \xi}{N}}}_{F(\xi)} H(\xi) = F(\xi)H(\xi) = G(\xi).
\end{aligned}
$$

# Convolution Theorem

$$
\begin{tikzcd}
g(t) = f(t) \star h(t) \arrow[r, dashed] \arrow[d, "FT"'] & f(t) \\
G(\xi) = F(\xi) H(\xi) \arrow[r] & F(\xi) = \dfrac{G(\xi)}{H(\xi)} \arrow[u, "FT^{-1}"']
\end{tikzcd}
$$

Figure 17: Application of the convolution theorem

# Symmetry Property of Fourier Transform

## Theorem

*If $f(n)$ is a real valued discrete signal of length $N$, the Fourier transform $F(\xi)$ fulfills the symmetry property:*

$$F(\xi) = \bar{F}(N - \xi),$$

*where " $\bar{\ }$ " denotes the conjugate complex.*

# Symmetry Property of Fourier Transform

Using the property that for real numbers $a \in \mathbb{R}$ complex and conjugate complex number are identical $a = \bar{a}$, we have $f(n) = \bar{f}(n)$ and thus

$$\bar{F}(N-\xi) = \sum_{k=0}^{N-1} \bar{f}(k) e^{\frac{2\pi i k(N-\xi)}{N}} = \sum_{k=0}^{N-1} f(k) e^{\frac{-2\pi i k(N-\xi)}{N}}$$

The $N$-th unit roots further fulfill

$x^N - 1 = 0$

$$e^{\frac{2\pi i k \xi}{N}} = e^{\frac{2\pi i k(\xi + m\cdot N)}{N}}$$

where $m$ is an integer, and thus we get:

$$\bar{F}(N-\xi) = F(\xi).$$

# Some useful Properties of the Fourier Transform

| | spatial domain | frequency domain |
|---|---|---|
| scaling | $f(at)$ | $\frac{1}{\lvert a \rvert} F(\frac{\xi}{a})$ |
| shifting | $f(t - t_0)$ | $e^{-i\xi t_0} F(\xi)$ |
| symmetry | $-1/(2\pi) \cdot F(t)$ | $f(-\xi)$ |
| differentiation | $d^n f(t)/d\, t^n$ | $(i\,\xi)^n F(\xi)$ |

nice

Table 1: Summary of important properties of the Fourier transform

# Diagnostic Medical Image Processing

# Diagnostic Medical Image Processing

## 1 Flat Panel Image Receptors

- Concept of Flat Panel Image Receptors
- Problem Statement: Defect Pixel Interpolation
- Fourier Transform Revisited
- Defect Pixel Correction by Spatial Interpolation (Bi Lin Int.)
- Defect Interpolation by Band Limitation
- Defect Pixel Interpolation using Symmetry Properties
- Take Home Messages
- Further Readings

$O(N \log N)$

FT $\longrightarrow$ Cut Off

$\downarrow$

$FT^{-1}$ $O(N \log N)$

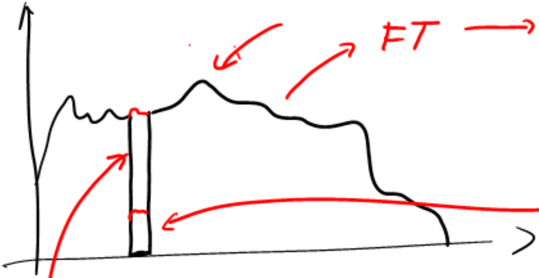

implies HUGE frequencies

SVD: $A = U\Sigma V^T$

$A\vec{x} = \vec{b}$

$\vec{x} = \underbrace{(A^TA)^{-1}A^T}\vec{b}$

$\left[\underbrace{(A^TA)}^{-1}A^T = V\Sigma^+U^T\right]$

$\underbrace{K(A^TA)}$

# DMIP

**Modalities**

DSA

Angio

Acquisition specific

Pre-processing

X-ray


- image intensifier (II)
- flat panel detector (FD)

Statistics

- Bootstrap (CV)
- fair parametrization

# Defect Interpolation by Band Limitation

The first idea for defect pixel interpolation using frequency domain methods is based on a fundamental result of signal theory:

- According to the sampling theorem the ideal signal $f(n)$ is required to be band-limited regarding to a certain band frequency $\xi$.
- Defect detector elements bring intensities of corresponding pixels down to zero.
- Defect pixels cause high differences in intensities of neighboring pixels and thus imply higher frequencies in the 2-D image function. These higher frequencies cause a violation of the required band limitation.

**Idea for defect interpolation:** Replace defect pixels iteratively by enforcing band limitation.

# Defect Interpolation by Band Limitation

| | |
|---|---|
| compute FT of input signal $g(n)$ | |
| | set $G(\xi) = 0$ for $\xi > B_\mathrm{u}$ or $\xi < B_\mathrm{l}$, |
| | compute inverse FT of corrected $G(\xi)$ |
| | Replace defect samples in $g(n)$ by values of inverse FT |
| UNTIL changes are below a threshold | |

Figure 18: Interpolation by enforcing a band limited signal in $[B_\mathrm{l}, B_\mathrm{u}]$

# Drawbacks of Band Limitation

The proposed method is quite simple and intuitive, but there exist a few serious practical issues:

e !

- Band limitation $B_{\mathrm{u}}, B_{\mathrm{v}}$ must be known
- The interpolation scheme is computationally expensive, because each iteration requires twice the Fourier transform of the signal. This prohibits its straightforward practical use.
- The proposed interpolation algorithm is not optimal w.r.t. minimum number of non-zero frequencies.
- Extrapolations decay outside observation interval
- The application of adaptive thresholding during interpolation is advantageous.

# Diagnostic Medical Image Processing

# Defect Pixel Interpolation

ideal

observed

mask [mähsk]

$f \cdot w = g$

**Observation:**

- $f(n)$, $g(n)$, $w(n)$ as previously defined are real valued signals.
- The images satisfy the following relationship:

$$g(n) = f(n) \cdot w(n) \quad \Leftrightarrow \quad G(\xi) = F(\xi) \star W(\xi) \tag{3}$$

- For the ideal, the mask, and the defect image, the Fourier transform satisfies the symmetry property:

$$\begin{aligned} F(\xi) &= \bar{F}(N - \xi) \\ G(\xi) &= \bar{G}(N - \xi) \\ W(\xi) &= \bar{W}(N - \xi) \end{aligned}$$

where the symbol $\bar{z}$ denotes the conjugate complex of $z$.

# Frequency Domain Defect Pixel Interpolation

We now we make explicit use of the symmetry property of the Fourier transform to derive an interpolation algorithm:

- Select a pair $\underbrace{G(s)}$ and $G(N-s)$ of the Fourier transform of the corrupted image showing pixels defects.
- Select a pair $\underbrace{F(s)}$ and $\underbrace{F(N-s)}$ of the Fourier transform of the ideal image.
- We can thus rewrite the Fourier transform using Dirac's $\delta$-function:

"^"

$$F(k) = \hat{F}(s)\delta(k-s) + \hat{F}(N-s)\delta(k-N+s)$$

where $\hat{F}$ denotes an estimate of $F$, and the $\delta$-function is defined by

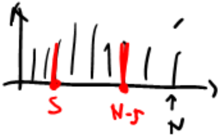


$$\delta(n) = \begin{cases} 1; & \text{if } n = 0 \\ 0.; & \text{otherwise} \end{cases}$$

CRAZY

# Frequency Domain Defect Pixel Interpolation

$f \cdot w = g$ $\qquad$ $F * W = G$ $\qquad$ $\mathrm{RMIP}_{\mathrm{RMMIP}}$

- Let us assume that the Fourier transform of the ideal image $F(k)$ consists only of two lines at $s$ and $N - s$, where $s \neq 0$. The convolution of image with Fourier transform of the given mask image $W$ leads to the Fourier transform of the observed corrupted image:

$$G(s) \quad = \quad F(s)W(0) + \hat{\hat{F}}(s)W(2s) \tag{4}$$

$$G(m) = F * W = \sum_{k=0}^{N} \hat{F}(k) \cdot W(m-k) = \hat{F}(s)\, W(m-s) + \hat{F}(N-s) \cdot W(m-N+s)$$

$$\underset{m=s}{G(s)} = F(s) \cdot W(0) + \hat{\hat{F}}(s) \cdot W(\underbrace{s - \cancel{N} + s}_{2s})$$

(I) $G(s) = \underbrace{\hat{F}(s)}_{?=a} \cdot W(0) + \underbrace{\hat{F}(s)}_{?=b} \cdot W(2s)$ $\boxed{x^{\nu} - 1 \equiv 0}$

(II) $\bar{G}(s) = \hat{F}(s) \cdot \bar{\omega}(0) + \hat{F}(s) \cdot \bar{\omega}(2s)$

$A\vec{x} = \vec{b}\ , \ \vec{x}, \vec{b} \in \mathbb{R}^2$

/

- For the conjugate complex Fourier transform of the observed image, we get:

$$\bar{G}(s) = \frac{1}{N}\left(\bar{\hat{F}}(s)\bar{W}(0) + \hat{F}(s)\bar{W}(2s)\right) \tag{5}$$

- Since $W$ is known, we get two equations linear in $\hat{F}(s)$ and $\bar{\hat{F}}(s)$. The final estimator for the Fourier transform of the ideal image:

$$\hat{F}(s) = N\frac{G(s)\bar{W}(0) - \bar{G}(s)W(2s)}{|W(0)|^2 - |W(2s)|^2}, \tag{6}$$

where $|.|$ is the absolute value of the complex number.

- An objective function to measure the quality of the interpolated image results from the least square error based on equation 2:

$$\Delta_\epsilon \quad = \quad \frac{1}{N}\sum_{n=0}^{N-1}(g(n) - w(n)\cdot f(n))^2 \tag{7}$$

- The spectrum of the error in the $i$-th iteration step is given by:

$$\underbrace{g^{(i)}(n)}_{\text{observation}} = g^{(i-1)}(n) \underbrace{- \frac{1}{N}\left[\hat{F}^{(i-1)}(s)\delta(n-s) + \hat{\hat{F}}^{(i-1)}(s)\delta(n-N+s)\right]} \tag{8}$$

# Interpolation Algorithm

| | | |
|---|---|---|
| compute FT of input signal $g(n)$ | | |
| Initialize $\hat{F}^0(k) = 0$, $G^0(k) = G(k)$, $i = 1$ | | |
| | Randomly select a line pair $s \neq 0$ $G^{i-1}(s) = G^{i-1}(N-s)$ | |
| | Estimate $\hat{F}^i(s)$, $\hat{F}^i(N-s)$ using (6) | |
| | Update spectrum $\hat{F}^i(k)$, compute error $\Delta_\epsilon$ using (8) | |
| | IF | error $\Delta_\epsilon$ above a threshold |
| | THEN Compute error spectrum $G^i(k)$, increment $i$ | |
| UNTIL error are below a threshold | | |
| Compute inverse FT of $\hat{F}^i(k)$ | | |

Figure 19: Interpolation due to Aach and Metzler [**?**]

# Interpolation Results

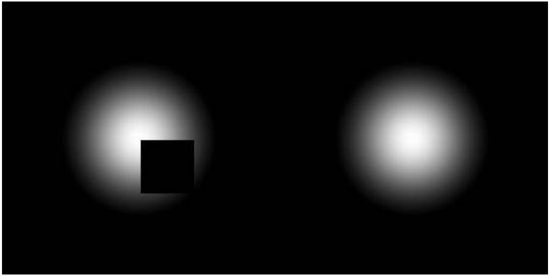

Figure 20: Synthetic image with a square artifact and the result of 100 iterations

# Interpolation Results

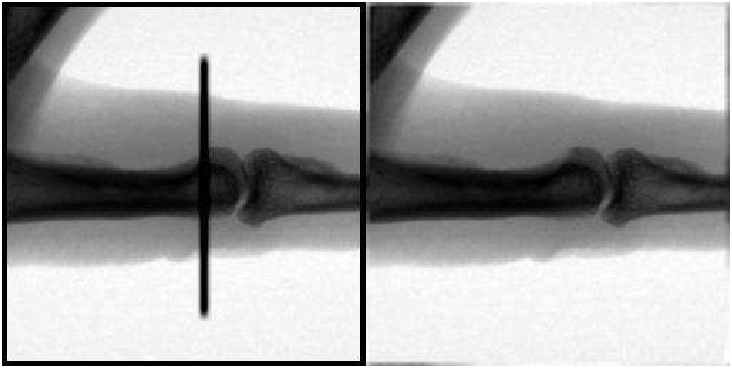

Figure 21: Original image including defects and the result after 500 iterations

# Interpolation Results

Figure 22: X-ray image with defects and the result of interpolation (500 iterations)

# Interpolation Results

Figure 23: X-ray image with defects and the result of interpolation (1000 iterations)

# Interpolation Results

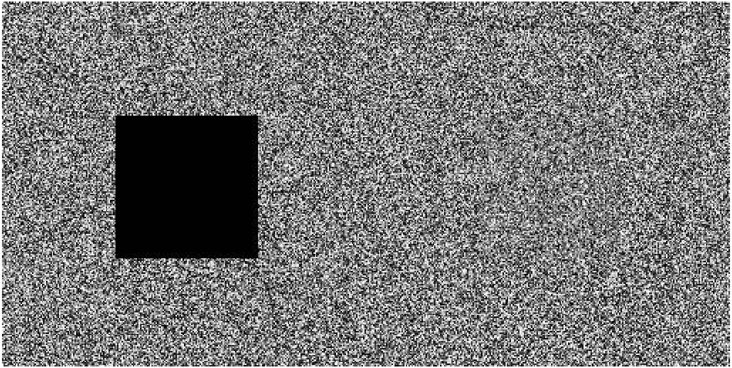

Figure 24: Artificial noise image with defect pixels and the result of interpolation (1000 iterations)

# Interpolation Results

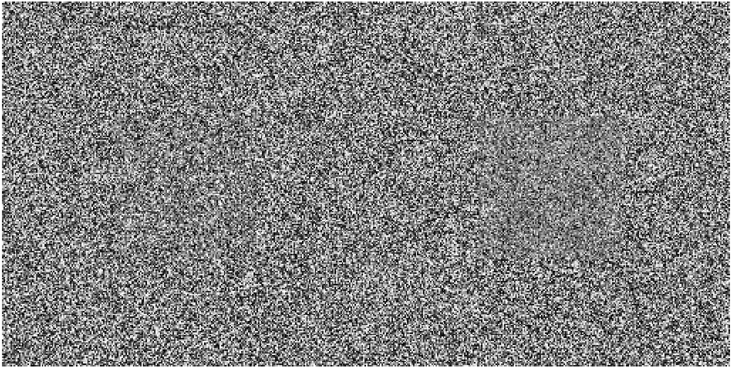

Figure 25: Result of interpolation after 1000 (left) and 5000 iterations (right)

# Application to Endoscopy

- endoscopy: wet surfaces lead to specular reflections
- segmentation of highlighted areas
- apply defect interpolation

Figure 26: Endoscopy image with reflections, segmentation result, result of interpolation (image: master thesis Xie Weiguo)

# Application to Ophthalmology

**Color images in Ophthalmology**

- In Ophthalmology the early diagnosis of diseases is done on the basis of retina images as shown, for instance, in Figure 17.
- For the diagnosis of Glaucoma disease, sometimes vessel structures are less important and misleading.

**Our approach to eliminate vessel structures:**

- Perform a segmentation of vessels, i.e. identify all image points that belong to a vessel.
- Consider pixels of vessels as defects.
- Run a defect pixel interpolation algorithm on images with defects.

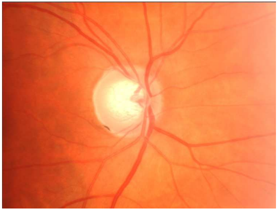

# Application to Ophthalmology

In Ophthalmology the early diagnosis of diseases is done on the basis of retina images as shown in Figure 17

# Application to Ophthalmology

In Ophthalmology the early diagnosis of diseases is done on the basis of retina images as shown in Figure 17

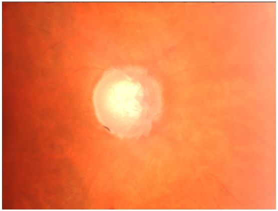

# Take Home Messages

- Flat panel detectors are standard in digital X-ray systems
- There exist different principles to realize a flat panel image receptor
- Defect pixel interpolation can be done in spatial and frequency domain.
- Be careful by applying defect pixel interpolation.
- Properties of Fourier transform.
- Applications of defect pixel interpolation to other problems in medical image processing.

# Further Readings

- Further details on flat panels can be found on the following web pages:
  - www.varian.com
  - www.trixell.com
- Basic information on DQE can be found in the origianal papers:
  - Albert Rose: A Unified Approach to the Performance of Photographic Film, Television Pickup Tubes, and the Human Eye, J. SMPE, 47, 273-294 (1946).
  - R. Clark Jones: On the Quantum Efficiency of Photographic Negatives, Photographic Science and Engineering, Vol. 2, No. 2, August, 1958, p. 57-65
- The method presented for defect pixel interpolation in the frequency domain was published in 2001 by Til Aach, Volker Metzler [**?**]
- X-ray imaging and image quality issues are discussed on the web-page http://lxi.leeds.ac.uk/.